JACS
JOURNAL OF THE AMERICAN CHEMICAL SOCIETY
pubs.acs.org/JACS
Article

Highly Nucleophilic Pyridinamide Anions in Apolar Organic Solvents due to Asymmetric Ion Pair Association

Veronika Burger, Maximilian Franta, Armin R. Ofial,* Ruth M. Gschwind,* and Hendrik Zipse*

Cite This: https://doi.org/10.1021/jacs.4c14825
Read Online

ACCESS | Metrics & More | Article Recommendations | Supporting Information

ABSTRACT: Free ions in organic solvents of low polarity would be valuable tools for the activation of low-reactivity substrates. However, the formation of unreactive ion pairs at concentrations relevant for synthesis has prevented the success of this concept so far. On the example of highly nucleophilic pyridinamide phosphonium salts in dichloromethane, we show that asymmetric aggregation offers a solution to this general problem. A combination of conductivity, diffusion-ordered NMR (DOSY), and kinetic measurements utilizing a refined ionic strength-controlled benzhydrylium ion methodology enables unique insight into the aggregation/association state of the ions and the nucleophilicity of the involved anions. This approach reveals that pyridinamide tetraphenylphosphonium salts aggregate in dichloromethane solution asymmetrically to form sandwich-type cations and anions together with their free counterions. The nucleophilicity of free pyridinamide ions exceeds that of the neutral reference nucleophile 9-azajulolidine (TCAP) by up to 2 orders of magnitude. Based on these results, we suggest that asymmetric aggregation in organic solvents of low polarity might be a general pathway to boost the reactivity of anionic nucleophiles.

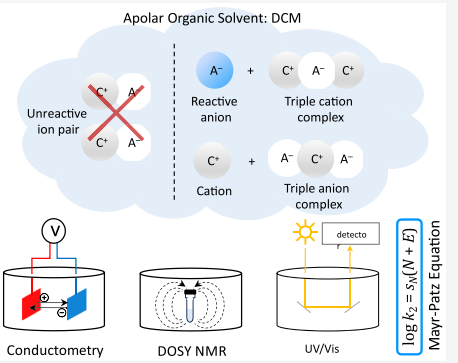

INTRODUCTION

Lewis basic pyridines, such as 4-(dimethylamino)pyridine (DMAP, **1**)[1] or the more reactive 9-azajulolidine (TCAP, **2**),[2] are frequently used catalysts for group transfer reactions such as acylations,[3−6] esterifications,[4,6] alkylations,[7] and silylations (Chart 1).[8,9] The nucleophilicity of these catalysts, together with other donor-substituted pyridines, has been quantified using Mayr's benzhydrylium ion method.[10−13] Even higher nucleophilicities and possibly also higher catalytic activities in Lewis base-mediated reactions may be expected for anionic Lewis bases. Given that anionic reagents unavoidably require a countercation, such salts tend to form ion pairs when dissolved in organic solvents of low polarity, such as dichloromethane (DCM).[14,15] This ion clustering has beneficially been used in ion pair catalysis,[16−18] which extends from classical cationic phase-transfer (PT) catalysis[19] to applications in asymmetric synthesis.[16,20−22] Recently, the Zipse group introduced Lewis basic pyridinamide ion pair catalysts, which outperformed TCAP and other neutral organocatalysts in selected catalytic benchmark reactions.[23,24]

Chart 1. Structures of Neutral Organocatalysts DMAP (1) and TCAP (2) and of Pyridinamide Ion Pair Catalysts 3a and 4a

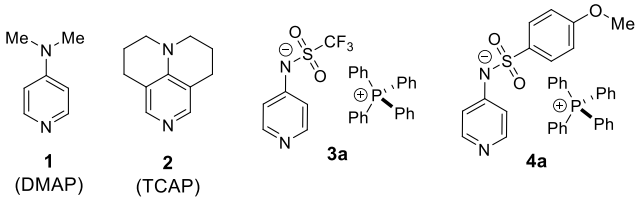

The pyridinamide phosphonium salts (such as **3a** and **4a** in Chart 1) investigated so far show the general usefulness of the concept of anionic nucleophilic organocatalysis, whose development tails that of neutral systems.[25−27]

In order to minimize ion pairing effects, most kinetic studies aiming at the quantification of the reactivity of anionic nucleophiles have been performed in highly polar solvents (water, DMSO, etc.), often in combination with crown ether additives to further reduce the interactions between metal counterions and the reacting anion.[28] In solvents of low polarity, the intrinsic nucleophilicity of a free anion should be far higher than that in more polar media. However, the reactivity of anions is attenuated by ion pair formation, which also gives rise to nonlinear effects and, thus, complicates systematic kinetic studies in organic solvents of low polarity [dichloromethane (DCM), tetrahydrofuran (THF), toluene, etc.] commonly employed in organocatalysis.

Received: October 23, 2024
Revised: December 9, 2024
Accepted: December 11, 2024
Published: January 24, 2025

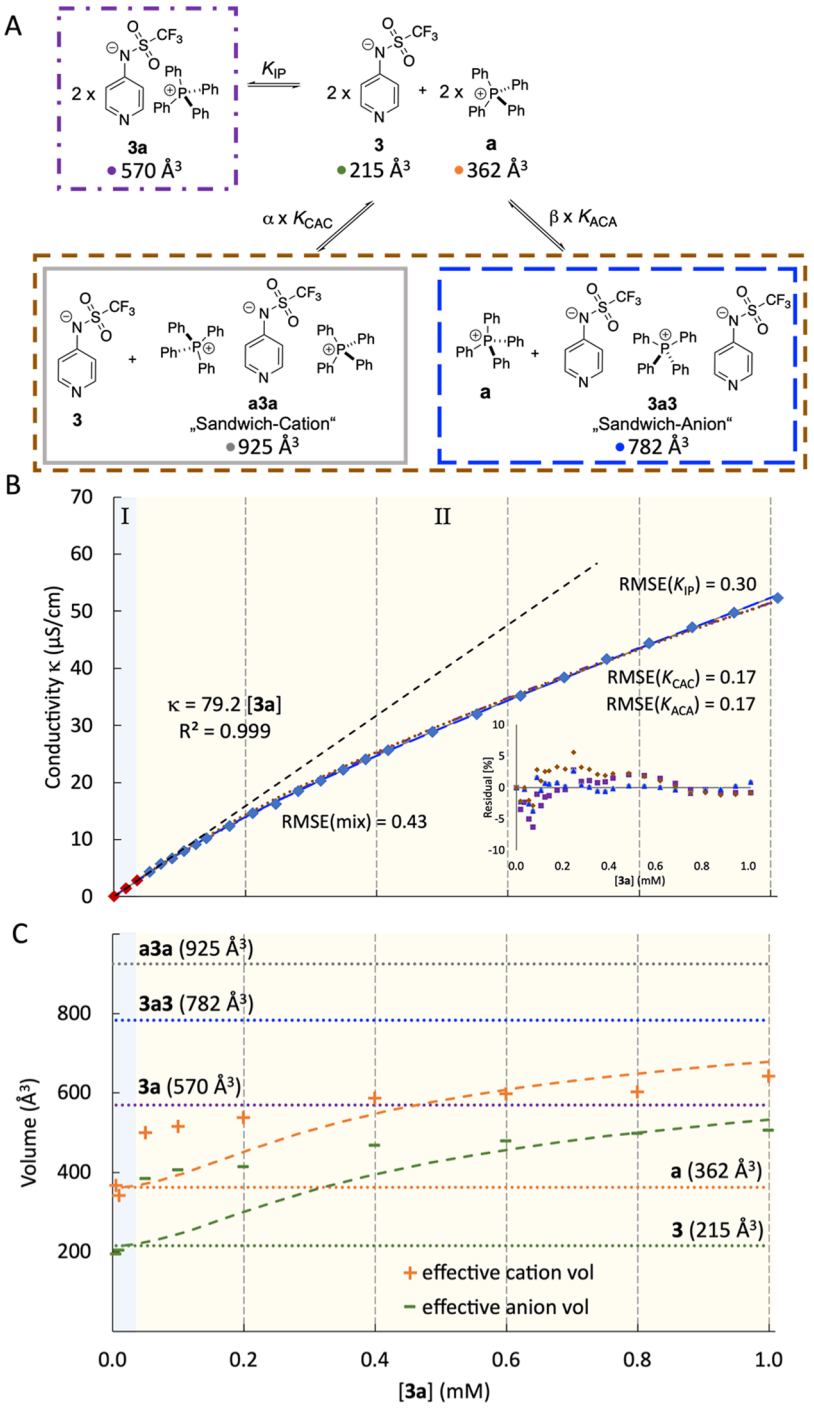

Figure 1. (A) 1:1 ion pair **3a**, sandwich cation **a3a**, and sandwich anion **3a3** as potential association models for anion **3** and cation **a** together with single-molecule dataset (SMD)-derived molecular volumes; (B) conductivity profile for **3a** in DCM fits to the calculated conductivity data for the 1:1 association model (purple dotted/dashed line), and the two sandwich association models (gray and blue line); (C) DOSY-derived ion volumes (in Å^3) compared to SMD-derived volumes (dashed horizontal lines) for single anion **3**, single cation **a**, ion pair **3a**, cation sandwich **a3a**, and anion sandwich **3a3**.

In order to elucidate the underlying principles responsible for the experimentally observed high nucleophilicity of the anions in salts such as **3a** and **4a**, we report here a combination of conductivity measurements, diffusion-ordered NMR (DOSY) measurements at very low concentrations, and photometric kinetic measurements by utilizing an ionic strength-controlled benzhydrylium methodology. This combination of physicochemical methods is expected to be generally applicable to ion pair chemistry and catalysis and may help to uncover the full potential of this field.

RESULTS AND DISCUSSION

Conductivity. Conductivity measurements have frequently been employed to quantify ion pairing effects.[29−32] This method was therefore applied to determine the association of the cationic and anionic components of phosphonium salt **3a** selected here as a reference system in DCM and acetonitrile

https://doi.org/10.1021/jacs.4c14825
J. Am. Chem. Soc. XXXX, XXX, XXX−XXX

(MeCN). In both solvents, **3a** is expected to be more reactive toward electrophiles than DMAP (**1**). Conductivity measurements were performed for concentrations ranging from 0.02 to 1.0 mM, as this appears to represent the onset of ion pair formation from free ions. At low electrolyte concentrations and for the case of noninteracting ions, the experimentally determined conductivity κ depends on the specific molar conductivity Λ_m and the ion concentration $[A]$, as expressed in eq 1.

$$\kappa = \Lambda_m[A] \quad (1)$$

In the polar aprotic solvent MeCN, the ions of **3a** are well stabilized and exist mainly as free ions, as indicated by a nearly perfect linear increase of conductivity with [**3a**] (see the SI, Figure S1). In the less polar solvent DCM, the situation is more complex, and two different domains can be seen in Figure 1B: (a) At low **3a** concentrations (region I, blue background, [**3a**] < 0.04 mM), the conductivity κ correlates linearly with [**3a**], and (b) a nonlinear part II at higher concentrations of **3a** (see Figure 1B beige background). While linear region I is assumed to represent the behavior of free anions (**3**) and cations (**a**), three ion association models were tested for nonlinear region II. The first corresponds to the formation of ion pair **3a** (purple box in Figure 1A), while the second model involves the formation of "sandwich cation" **a3a** together with free anion **3** (gray box in Figure 1A), and the third model considers the formation of an analogous sandwich anion **3a3** (blue box in Figure 1A). The latter model was originally proposed to account for the properties of tetraalkyl ammonium salts in apolar solution[33] and subsequently employed for a variety of systems in organic solvents.[34−37] In order to compare both models on equal footing, the respective equilibrium constants K_{IP} and K_{CAC} are defined relative to two equivalents, each of free cation **a** and free anion **3**.

The 1:1 ion pair model retains the specific molar conductivity Λ_m derived from the linear region I and adds the effects of reducing the number of conducting species through the formation of overall neutral (and thus inactive) ion pairs **3a**. Fitting this model to the observed conductivities up to an overall concentration of 1.0 mM yields ion pair formation constant $K_{IP} = 6.86 \times 10^5$ M^{-2} with good accuracy. The second model involves the formation of sandwich cation **a3a** together with one equivalent of free anion **3** (gray box in Figure 1A), again combined with the specific molar conductivity Λ_m value obtained from the linear region I. This model fits the observed conductivity values in the region up to 1.0 mM with a sandwich association constant $K_{CAC} = 6.38 \times 10^6$ M^{-2} with equally good accuracy. This is also true for the third model involving the formation of sandwich anion **3a3** (blue box in Figure 1A), for which the optimized association constant is $K_{ACA} = 6.38 \times 10^6$ M^{-2}, numerically identical with K_{CAC}. The measured conductivity values, together with the model predictions, are depicted in Figure 1B (gray line for the **a3a** sandwich model, blue line for the **3a3** sandwich model, and purple dotted line for the 1:1 ion pair), which illustrates that all models fit the experimental conductivity curve equally well, as indicated by largely similar RMSE values of RMSE(K_{CAC}) = 0.17, RMSE(K_{ACA}) = 0.17, and RMSE(K_{IP}) = 0.30, respectively.

DOSY-NMR. Since conductivity measurements alone cannot provide direct information on the size of the contributing ions, DOSY-NMR measurements of **3a** were performed in DCM-d_2 for concentrations ranging from 0.005 to 1.0 mM (see Figure 1C and SI, Chapter 4 for detailed information). To enable DOSY measurements at these low concentrations, a 600 MHz spectrometer with a helium cryo probe and measurement times up to 16 h per sample were employed. The DOSY results were compared to calculated volumes of anion **3** (215 Å^3), cation **a** (362 Å^3), and contact ion pair **3a** (570 Å^3), which are based on the van der Waals cavities employed in the SMD continuum solvation model at the SMD(DCM)/B3LYP-D3/6-31+G(d) level of theory and indicated through the horizontal dashed lines in Figure 1C. At [**3a**] = 0.005 mM as the lowest concentration accessible for DOSY measurements, we determined volumes of 367 Å^3 for cation **a** and 192 Å^3 for anion **3**, both of which agree closely with the SMD-derived volumes for cation **a** and anion **3**. At any concentration of **3a** > 0.005 mM, considerably larger cation and anion volumes were observed already in region I (for full data, see the SI, Chapter 4). In the 1:1 association model shown in the purple box in Figure 1A, the volumes of both species are expected to converge to the SMD-derived value of 570 Å^3 for 1:1 ion pair **3a**. Instead, we persistently detected substantially different effective volumes for cation **a** and anion **3** also at higher concentrations (region II), and we also note that the DOSY-derived volume for the cationic species exceeds that calculated for the 1:1 ion pair **3a**.

This latter observation can be rationalized with the sandwich ion models, where the DOSY-derived cation volume is expected to approach that of the **a3a** sandwich cation of 925 Å^3. Combining the SMD-derived molecular volumes of ions with the equilibrium constants obtained from conductivity measurements allows us to predict concentration-dependent effective cation and anion volumes. These are shown in Figure 1C as a green line for the anion and an orange line for the cation volumes. Comparing experimentally derived with theoretically predicted volumes shows these to coincide quite well between 0.4 and 1.0 mM for the cation sandwich model.[38] In contrast, the 1:1 model predicts volumes for both ions, which are significantly lower than the experimental values (by more than 200 Å^3 for the cation and >100 Å^3 for the anion; see the SI). This is also true for the **3a3** anion sandwich model that predicts larger anion than cation volumes, not consistent with the DOSY experiments. The agreement between experimentally determined DOSY volumes and model predictions can be further improved by combining the two sandwich models considered here. This requires optimization of the two scaling factors α and β shown in Figure 1A, such that the agreement with the conductivity data and the DOSY volumes is optimized. The best agreement for ion pair **3a** is found for α = 0.44 and β = 0.21, which implies that 50% of the anion **3** is free while the other 50% is stored in the two sandwich complexes at I = 1.0 mM. In contrast, the DOSY experiments for **4a** show inverted relative ion volumes with larger values for the anionic species (see the SI, Chapter 4). This is reflected by the mixing coefficients for salt **4a** amounting to α = 0.12 and β = 0.61. This implies that 34% of anion **4** is free, and 66% is hidden in the two sandwich complexes. The performance of these "mixed sandwich" models is quite satisfactory in concentration region II but less so in region I with its rapid increase of ion volumes with salt concentration. It is an intriguing aspect of the formation of sandwich cation **a3a** that it generates one equivalent of free anion **3** as the counterion. The concentration of free anion **3** will quite obviously impact the efficiency of pyridinamide anion-based catalytic systems,

https://doi.org/10.1021/jacs.4c14825
J. Am. Chem. Soc. XXXX, XXX, XXX−XXX

where free anion **3** is expected to account for most of the observed activity.

Kinetics. To characterize the nucleophilic reactivity of **3a** and **4a** in an organic solvent of low polarity, such as DCM, we refined Mayr's well-known benzhydrylium ion method by implementing an ionic strength control. This enabled the characterization of free anionic nucleophiles for the first time in DCM. Mayr's methodology has repeatedly demonstrated its utility to describe the reactivity of a wide range of carbon-, nitrogen, oxygen-, sulfur-, and phosphor-based nucleophiles in different solvents,[39] including DMAP (**1**) and TCAP (**2**).[10,11,39] In short, the benzhydrylium ion method involves the photometric monitoring of the reactions of colored benzhydrylium salts, such as **5a**–**c** (Table 1), whose

Table 1. Second-Order Rate Constants k_2 for the Reactions of DMAP (1), TCAP (2), and Pyridinamide Salts 3a and 4a with Reference Electrophiles 5a, 5b, and 5c in MeCN (at 20 °C) Analyzed by Equation 3 to Give the Nucleophile-Specific Reactivity Parameters N (and s_N)

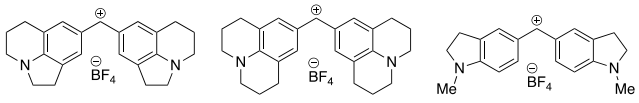

(lil)$_2$CH$^+$ (**5a**) E = -10.04 (jul)$_2$CH$^+$ (**5b**) E = -9.45 (ind)$_2$CH$^+$ (**5c**) E = -8.76

	k_2 [M^{-1} s^{-1}]			
cat	**5a**	**5b**	**5c**	N (s_N)
1[a]	2.11 × 10^3	5.30 × 10^3	1.29 × 10^4	15.51 (0.62)[e]
2[b]	6.30 × 10^3		4.17 × 10^4	15.60 (0.68)[e]
3[c]	7.16 × 10^3	1.53 × 10^4	4.13 × 10^4	16.38 (0.60)
4[d]	5.11 × 10^4	1.36 × 10^5	3.47 × 10^5	17.28 (0.65)

[a]Second-order rate constants k_2 from ref 10. [b]Second-order rate constants k_2 from ref 11. [c]Assuming that [**3**] = [**3a**]$_0$. [d]Assuming that [**4**] = [**4a**]$_0$. [e]Additional k_2 values from refs 10,11 were used to determine N (and s_N).

electrophilic reactivities are characterized by the solvent-independent parameters E, with nucleophiles used in excess concentration to achieve kinetics under pseudo-first-order conditions. The first-order rate constants k_{obs} (s^{-1}) can then be obtained by fitting a monoexponential decay function to the decreasing absorption of **5** during the reaction with **3**. The conductivity measurements (see the SI, Figure S1) showed that **3a** and **4a** fully dissociate into anions and cations when dissolved in MeCN. Accordingly, a linear increase of pseudo-first-order rate constants k_{obs} with nucleophile concentrations [**3**] (or [**3a**]) was observed in the kinetics of reactions of **3a** with **5** (eq 2).

$$k_{obs} = k_2[\mathbf{3}] \quad (2)$$

$$\log k_2 = s_N(N + E) \quad (3)$$

Equation 2 thus yields second-order rate constants k_2 (M^{-1} s^{-1}) for the reactions of **3** with **5a**–**c** in acetonitrile (Table 1). The rate constants k_2 for **3** are approximately three times larger than those for analogous reactions of **5** with DMAP (**1**) and quite similar to those for reactions with TCAP (**2**). Analyzing the kinetic data with the Mayr–Patz eq 3 yields the nucleophilicity N = 16.38 (s_N = 0.60) of **3** in MeCN. Following the same approach for **4a** yields N(**4a**) = 17.28 (s_N = 0.65), in excellent agreement with the results obtained for these two systems in selected catalytic transformations.[23]

The kinetics of reactions of **3a** with reference electrophiles **5** in DCM solution, however, showed a more complex dependence of k_{obs} on [**3a**] in the concentration range from 0.01 to 1.0 mM (red and blue diamonds in Figure 2). In analogy to the conductivity measurements, an initial region I with linear k_{obs} vs [**3a**]$_0$ relation was observed (Figure 2, blue background, experimental values marked in red). At higher [**3a**] values, this is followed by nonlinear region II (blue diamonds on a beige background in Figure 2), where the observed rate constants deviate negatively from the linear correlation extrapolated from region I. The degree of deviation reflects the fraction of anion **3** captured in the (presumably) unreactive sandwich cation **a3a** and the (presumably) less reactive sandwich anion **3a3**.

Analysis of the kinetic data in region I (0.01–0.03 mM) is straightforward, as conductivity measurements in combination with the sandwich association models indicate almost complete (>97%) dissociation into separate ions **3** and **a**, that is, [**3**] = [**3a**]$_0$. Application of eq 2 then yields k_2(**5a**) = 1.84 × 10^6 M^{-1} s^{-1}, as indicated by the dashed line in Figure 2.

In synthetic applications, the concentration of ion pair catalysts is usually 1.0 mM or higher, which is far into the nonlinear region II. Increasing ion concentrations may impact the reaction rates not only through shifting the association equilibrium toward a higher fraction of ionic aggregates but also through nonspecific polarity effects. To assess the influence of the high salt concentration on the solvent polarity, we determined Reichardt's E_T(30) values in DCM solutions with increasing concentrations of pyridinamide salt **3a** and additive Ph$_4$P$^+$BF$_4^-$ (**6**). As shown in Figure 2, this additive combines the common unreactive ions in the reaction mixture, that is, the BF$_4^-$ of the benzhydrylium salts and the unreactive Ph$_4$P$^+$ countercation of the pyridinamide salts. We observed insignificant changes of the E_T(30) values even at total salt concentrations of up to 6.0 mM (see the SI).

We conclude, therefore, that addition of **6** to a reaction mixture of **3a** and **5a**–**c** does not change the overall polarity of the solvent system and affects only the position of the ion pairing equilibrium shown in Figure 2, where higher concentrations of Ph$_4$P$^+$ (=**a**) give rise to an increase of [**a3a**]. To further investigate the effect of the Ph$_4$P$^+$BF$_4^-$ (**6**) additive, the ion volumes of selected **3a** + **6** mixtures were determined by DOSY measurements. The DOSY experiments show that the volumes of the cation and anion determined for **3a** + **6** mixtures at an ionic strength of I = 1.0 mM are in the same region as the volumes obtained for a pure **3a** solution at [**3a**] = 1.0 mM (for details, see the SI).[40] The kinetics of the reaction of **3a** + **5a** was subsequently studied at a constant ionic strength (I) of I = 1.0 mM, as this represents the highest concentration of **3a** in this study. At [**3a**] < 1.0 mM, the ionic strength of the DCM solution was adjusted by addition of **6** such that in each kinetic measurement, the condition [**3a**] + [**6**] + [**5a**] = 1.0 mM is fulfilled. By maintaining I = 1.0 mM, the rate constants k_{obs} for **3a** + **5a** reactions in DCM correlated linearly with [**3a**] in the entire concentration range from 0.01 to 1.0 mM (turquoise points in Figure 2). When we account for the fact that variable fractions of anion **3** are caught in unreactive sandwich cation **a3a** (and to a smaller extent also in anion sandwich **3a3**) and also consider the effect of additive **6** on [Ph$_4$P$^+$], we obtain k_2(**5a**) = 5.42 × 10^5 M^{-1} s^{-1} for the reaction of **3** with **5a**, which is by a factor of 3.5 lower than k_2 obtained in the low-concentration (LC) region (Table 2). Analogous kinetic measurements at I = 1.0 mM were

https://doi.org/10.1021/jacs.4c14825
J. Am. Chem. Soc. XXXX, XXX, XXX–XXX

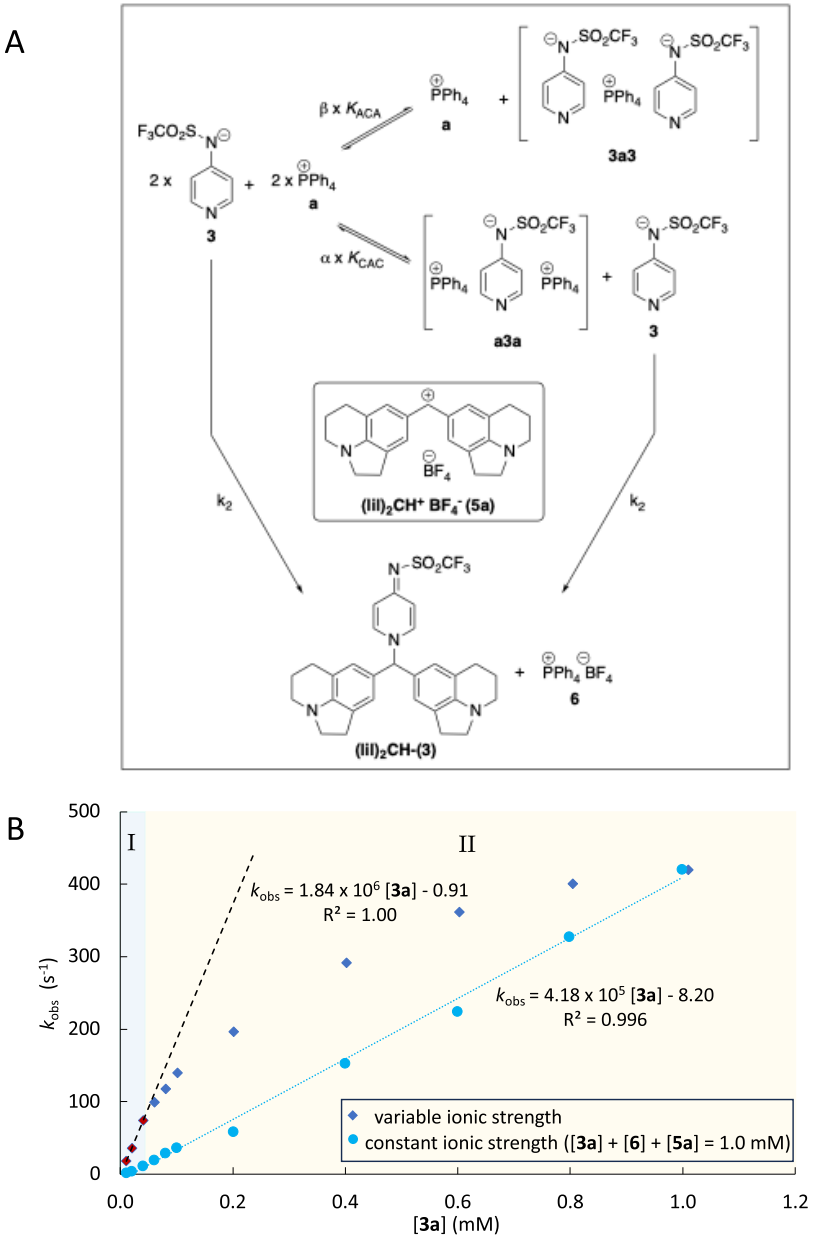

Figure 2. (A) Benzhydrylium ion reaction applied for the quantification of the nucleophilicity of **3**. (B) Correlation of k_{obs} for the reaction of **5a** with **3a** for salt concentrations [**3a**] from 0.01 to 1.0 mM in DCM at 20 °C (blue diamonds) and in the presence of additive PPh_4BF_4 (**6**) (turquoise dots).

performed for reactions of **3a** with more reactive benzhydryl salts **5b** and **5c** (Table 2).

In DCM as the solvent, we note a moderate increase in the bimolecular rate constants k_2 when going from DMAP (**1**) to TCAP (**2**) but a significantly larger increase of the k_2 values for **3a** (Table 2). The k_2 values for the reaction of **3a** with **5a−c** in DCM in the low-concentration (LC) region I (as defined in Figure 2) exceed those for **2** by approximately 2 orders of magnitude. Analyzing the LC kinetic data by the Mayr−Patz equation in eq 3 gives N = 17.78 (s_N = 0.81) for **3a**. Rate constants k_2 for reactions of **3** with all three benzhydryl cations **5a−c** decrease slightly (by a factor of 3.5−4.5) under conditions of constant ion strength (I = 1.0 mM). The resulting N-parameter for **3** is, however, hardly changed at N = 17.88 (s_N = 0.73). Following the same mode of analysis for **4a** under reaction conditions where I = 1.0 mM, we find that anion **4** exceeds the nucleophilicity of **3** by a factor of 3.0 ± 0.5 in its reaction with benzhydryl cations **5a−c**, which is also reflected in the respective nucleophilicity parameter of N(**4**) = 19.63 (s_N = 0.65).

These measurements thus establish **3a** and **4a** as potent and highly nucleophilic pyridine derivatives in solvents of low polarity (Figure 3). That **4a** is more nucleophilic than **3a** is in full agreement with the results for selected organocatalytic transformations performed in $CDCl_3$ as the solvent.[23] The combined methodology developed here thus allows for a quantitative assessment of catalyst nucleophilicity at synthetically relevant concentrations.

CONCLUSIONS

Pyridinamide salts **3a** and **4a** exceed the nucleophilic reactivity of the highly reactive neutral Lewis base TCAP (**2**) by up to 2

https://doi.org/10.1021/jacs.4c14825
J. Am. Chem. Soc. XXXX, XXX, XXX−XXX

Table 2. Second-Order Rate Constants k_2 of the Reactions of DMAP (1), TCAP (2), and Pyridinamide Salt 3a with Reference Electrophiles 5a, 5b, and 5c in DCM (at 20 °C)

	k_2 [M^{-1} s^{-1}]		
cat	5a	5b	5c
1[a]	6.45×10^3	9.84×10^3	4.96×10^4
2[b]	1.42×10^4	3.11×10^4	1.28×10^5
3[c]	1.84×10^6 (LC)	4.23×10^6 (LC)	1.98×10^7 (LC)
3[d]	5.42×10^5 (mix)	1.25×10^6 (mix)	4.64×10^6 (mix)
4[e]	1.69×10^6 (mix)	4.19×10^6 (mix)	1.15×10^7 (mix)

[a]Second-order rate constants k_2 from ref 10a. [b]This work, see the Supporting Information for details of the kinetic experiments. [c]Determined at [3] < 0.03 mM, that is, in the low-concentration (LC) region I (Figure 2), by assuming [3] = $[3a]_0$. [d]Determined over a concentration range [3a] = 0.1 to 0.3 mM at constant ionic strength I = 1.0 mM (kept by addition of salt 6) by assuming a mixed sandwich association model (see the SI for details). [e]Determined over a concentration range [4a] = 0.04 to 0.1 mM at constant ionic strength I = 1.0 mM (kept by addition of salt 6) by assuming a mixed sandwich association model.

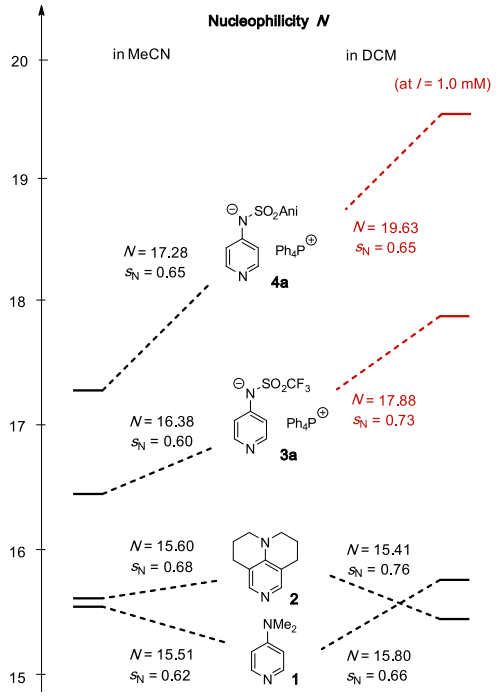

Figure 3. Mayr nucleophilicities N (and s_N) of DMAP (1), TCAP (2), and pyridinamide anions 3 and 4 (Ani = *p*-methoxyphenyl) in MeCN and DCM.

orders of magnitude in DCM. Employing a combination of conductivity and DOSY measurements, we have deciphered an asymmetric association behavior of both pyridinamide ion pairs in the low polarity solvent DCM, which includes both cationic and anionic sandwich complexes but not the commonly assumed and unreactive 1:1 ion pair. Without the combination of conductivity and DOSY measurements, this result could not have been achieved since conductivity alone does not give insight into the type of charged species that are being measured. The reactivity of the supernucleophilic anions 3 and 4 was quantified with the newly developed ionic strength-controlled benzhydrylium ion method, which facilitates the comparison of 3a and 4a with neutral nucleophilic catalysts, such as DMAP or TCAP. In DCM, we were able to evaluate kinetic data not only at low salt concentrations but also at synthetically relevant higher concentrations by keeping the ionic strength constant throughout the measurement to prevent the interference of ion association. The direct comparison of k_2 values for reactions with cationic reference electrophiles reveals reactivity values of pyridinamide anions 3 and 4 (at high concentration) that are 39 and 90 times higher than that of TCAP (2). The superior reactivity of pyridinamide anions 3 and 4 has recently been observed in catalytic reactions with isocyanates and Michael acceptors as electrophiles.[23,24] This indicates that the higher nucleophilicity of 3 and 4 in comparison to neutral nucleophilic catalysts might be comparably effective for reactions with neutral electrophiles in low polarity media (alkanes, THF, and Et_2O). The asymmetric ion association described here opens the general avenue for employing highly reactive free anions to activate so far inaccessible substrates in catalytic transformations.

■ ASSOCIATED CONTENT

Supporting Information

The Supporting Information is available free of charge at https://pubs.acs.org/doi/10.1021/jacs.4c14825.

Additional experimental and computational details, analysis procedures, and methods, including step by step descriptions (PDF)

Accession Codes

CCDC accession codes 2310788−2310789 contain the supplementary crystallographic data for this paper. These data can be obtained free of charge via www.ccdc.cam.ac.uk/data_request/cif, by emailing data_request@ccdc.cam.ac.uk, or by contacting the Cambridge Crystallographic Data Centre, 12 Union Road, Cambridge CB2 1EZ, UK; fax: + 44 1223 336033.

■ AUTHOR INFORMATION

Corresponding Authors

Armin R. Ofial − *Department of Chemistry, Ludwig-Maximilians-Universität München, 81377 München, Germany*; Email: ofial@lmu.de

Ruth M. Gschwind − *Institute for Organic Chemistry, University Regensburg, 93053 Regensburg, Germany*; Email: ruth.gschwind@ur.de

Hendrik Zipse − *Department of Chemistry, Ludwig-Maximilians-Universität München, 81377 München, Germany*; orcid.org/0000-0002-0534-3585; Email: zipse@cup.uni-muenchen.de

Authors

Veronika Burger − *Department of Chemistry, Ludwig-Maximilians-Universität München, 81377 München, Germany*

Maximilian Franta − *Institute for Organic Chemistry, University Regensburg, 93053 Regensburg, Germany*

Complete contact information is available at: https://pubs.acs.org/10.1021/jacs.4c14825

Author Contributions

The manuscript was written through contributions of all authors. All authors have given approval to the final version of the manuscript.

https://doi.org/10.1021/jacs.4c14825
J. Am. Chem. Soc. XXXX, XXX, XXX−XXX

Notes

The authors declare no competing financial interest.

■ ACKNOWLEDGMENTS

This work was funded by the Deutsche Forschungsgemeinschaft (DFG, German Research Foundation)-426795949 through the Research Training Group (RTG) 2620 "Ion Pair Effects in Molecular Reactivity." The authors are thankful to Dr. Robert J. Mayer (LMU) for help with the conductivity measurements, Nathalie Hampel (LMU) for the synthesis of **5a−c**, Dr. Fabian Zott (LMU) for help with kinetics simulations, and Christian Scholtes (RU) for providing a Python script for the DOSY evaluation.

■ REFERENCES

(1) (a) Litvinenko, L. M.; Kirichenko, A. I. Basicity and Stereospecificity in Nucleophile Catalysis by Tertiary Amines. *Dokl. Akad. Nauk. SSSR* **1967**, *176*, 97−100. (b) Steglich, W.; Höfle, G. N,N-Dimethyl-4-pyridinamine, a Very Effective Acylation Catalyst. *Angew. Chem., Int. Ed.* **1969**, *8* (12), 981.

(2) Heinrich, M. R.; Klisa, H. S.; Mayr, H.; Steglich, W.; Zipse, H. Enhancing the Catalytic Activity of 4-(Dialkylamino)Pyridines by Conformational Fixation. *Angew. Chem., Int. Ed.* **2003**, *42* (39), 4826−4828.

(3) Steglich, W.; Höfle, G. Über eine einfache darstellung von acyl-oxazolinonen-(5) aus 5-acyloxy-oxazolen II. Mitteilung über hypernucleophile acylierungskatalysatoren. *Tetrahedron Lett.* **1970**, *11* (54), 4727−4730.

(4) Hassner, A.; Alexanian, V. Direct room temperature esterification of carboxylic acids. *Tetrahedron Lett.* **1978**, *19* (46), 4475−4478.

(5) Höfle, G.; Steglich, W.; Vorbrüggen, H. 4-Dialkylaminopyridines as Highly Active Acylation Catalysts. *Angew. Chem., Int. Ed.* **1978**, *17*, 569−583.

(6) Neises, B.; Steglich, W. Simple Method for the Esterification of Carboxylic Acids. *Angew. Chem., Int. Ed.* **1978**, *17* (7), 522−524.

(7) Chaudhary, S. K.; Hernandez, O. A Simplified Procedure for the Preparation of Triphenylmethylethers. *Tetrahedron Lett.* **1979**, *20* (2), 95−98.

(8) Patschinski, P.; Zhang, C.; Zipse, H. The Lewis Base-Catalyzed Silylation of Alcohols-a Mechanistic Analysis. *J. Org. Chem.* **2014**, *79* (17), 8348−8357.

(9) Chaudhary, S. K.; Hernandez, O. 4-Dimethylaminopyridine: An Efficient and Selective Catalyst for the Silylation of Alcohols. *Tetrahedron Lett.* **1979**, *20* (2), 99−102.

(10) For the nucleophilic reactivity of DMAP (**1**) in MeCN, see: (a) Brotzel, F.; Kempf, B.; Singer, T.; Zipse, H.; Mayr, H. Nucleophilicities and Carbon Basicities of Pyridines. *Chem. - Eur. J.* **2007**, *13* (1), 336−345. For supplementary kinetic data and revised *N* (and s_N) parameters for DMAP (**1**), see: (b) Nigst, T. A.; Ammer, J.; Mayr, H. Photogeneration of Benzhydryl Cations by Near-UV Laser Flash Photolysis of Pyridinium Salts. *J. Phys. Chem. A* **2012**, *116* (33), 8494−8499.

(11) Tandon, R.; Unzner, T.; Nigst, T. A.; De Rycke, N.; Mayer, P.; Wendt, B.; David, O. R. P.; Zipse, H. Annelated Pyridines as Highly Nucleophilic and Lewis Basic Catalysts for Acylation Reactions. *Chem. - Eur. J.* **2013**, *19* (20), 6435−6442.

(12) Mayr, H. Reactivity scales for quantifying polar organic reactivity: the benzhydrylium methodology. *Tetrahedron* **2015**, *71*, 5095−5111.

(13) Lakhdar, S. *Lewis Base Catalysis in Organic Synthesis*, 1st ed.; Vedejs, E.; Denmark, S. E., Eds.; Wiley-VCH: Weinheim, 2016; Chapter 4, pp 85−116.

(14) Marcus, Y.; Hefter, G. Ion Pairing. *Chem. Rev.* **2006**, *106* (11), 4585−4621.

(15) Reichardt, C. *Solvents and Solvent Effects in Organic Chemistry*, 3rd ed.; VCH: Weinheim, 2003; Chapter 5.5.5.

(16) Brak, K.; Jacobsen, E. N. Asymmetric Ion-Pairing Catalysis. *Angew. Chem., Int. Ed.* **2013**, *52* (2), 534−561.

(17) (a) Waser, M.; Novacek, J.; Gratzer, K. Cooperative Catalysis Involving Chiral Ion Pair Catalysts. In *Cooperative Catalysis*; Peters, R., Ed.; Wiley-VCH: Weinheim (Germany), 2015; Chapter 7, pp 197−226. (b) Otevrel, J.; Waser, M. Asymmetric Phase-Transfer Catalysis—From Classical Application to New Concepts. In *Asymmetric Organocatalysis: New Strategies, Catalysts, and Opportunities*, Albrecht, Ł.; Albrecht, A.; Dell'Amico, L., Eds.; Wiley-VCH, 2023; Chapter 3, pp 71−120.

(18) Ye, X.; Tan, C. H. Enantioselective Transition Metal Catalysis Directed by Chiral Cations. *Chem. Sci.* **2021**, *12* (2), 533−539.

(19) Shirakawa, S.; Maruoka, K. Recent Developments in Asymmetric Phase-Transfer Reactions. *Angew. Chem., Int. Ed.* **2013**, *52* (16), 4312−4348.

(20) Merten, C.; Pollok, C. H.; Liao, S.; List, B. Stereochemical Communication within a Chiral Ion Pair Catalyst. *Angew. Chem., Int. Ed.* **2015**, *54* (30), 8841−8845.

(21) Mahlau, M.; List, B. Asymmetric Counteranion-Directed Catalysis: Concept, Definition, and Applications. *Angew. Chem., Int. Ed.* **2013**, *52* (2), 518−533.

(22) Phipps, R. J.; Hamilton, G. L.; Toste, F. D. The Progression of Chiral Anions from Concepts to Applications in Asymmetric Catalysis. *Nat. Chem.* **2012**, *4* (8), 603−614.

(23) Helberg, J.; Ampßler, T.; Zipse, H. Pyridinyl Amide Ion Pairs as Lewis Base Organocatalysts. *J. Org. Chem.* **2020**, *85*, 5390−5402.

(24) Dempsey, S. H.; Lovstedt, A.; Kass, S. R. Electrostatically Enhanced 3- and 4-Pyridyl Borate Salt Nucleophiles and Bases. *J. Org. Chem.* **2023**, *88* (15), 10525−10538.

(25) Dale, H. J. A.; Hodges, G. R.; Lloyd-Jones, G. C. Kinetics and Mechanism of Azole N−π^*-Catalyzed Amine Acylation. *J. Am. Chem. Soc.* **2023**, *145* (32), 18126−18140.

(26) Yang, X.; Birman, V. B. Acyl Transfer Catalysis with 1,2,4-Triazole Anion. *Org. Lett.* **2009**, *11* (7), 1499−1502.

(27) Mai, B. K.; Koenigs, R. M.; Nguyen, T. V.; Lyons, D. J. M.; Empel, C.; Pace, D. P.; Dinh, A. H. Tropolonate Salts as Acyl-Transfer Catalysts under Thermal and Photochemical Conditions: Reaction Scope and Mechanistic Insights. *ACS Catal.* **2020**, *10* (21), 12596−12606.

(28) Liotta, C. L.; Harris, H. P. The Chemistry of "Naked" Anions. I. Reactions of the 18-Crown-6 Complex of Potassium Fluoride with Organic Substrates in Aprotic Organic Solvents. *J. Am. Chem. Soc.* **1974**, *96*, 2250−2252.

(29) Coury, L. Conductance Measurements Part 1: Theory. *Current* **1999**, *3* (2), 91−96.

(30) Mizuhata, M. Electrical Conductivity Measurement of Electrolyte Solution. *Electrochemistry* **2022**, *90* (10), 1−12.

(31) Martínez, L. Measuring the Conductivity of Very Dilute Electrolyte Solutions, Drop by Drop. *Quim. Nova* **2018**, *41* (7), 814−817.

(32) Schneider, R.; Mayr, H.; Plesch, P. H. Ionisation and Dissociation of Diarylmethyl Chlorides in BCl_3/CH_2Cl_2 Solution: Spectroscopic Evidence for Carbenium Ion Pairs. *Ber. Bunsenges. Phys. Chem.* **1987**, *91*, 1369−1374.

(33) The triple ion sandwich model has first been proposed in: Fuoss, R. M.; Kraus, C. A. Properties of Electrolytic Solutions. IV. The Conductance Minimum and the Formation of Triple Ions Due to the Action of Coulomb Forces. *J. Am. Chem. Soc.* **1933**, *55*, 2387−2399.

(34) Jiang, J.; Dennis, K. P. N. G. A Decade Journey in the Chemistry of Sandwich-Type Tetrapyrrolato-Rare Earth Complexes. *Acc. Chem. Res.* **2009**, *42* (1), 79−88.

(35) Hojo, M.; Moriyama, H. Conductance in Isodielectric Mixed Solvents Containing Triple Ions. *J. Solution Chem.* **1996**, *25* (7), 681−694.

(36) Hojo, M.; Ueda, T.; Inoue, T.; Ike, M.; Kobayashi, M.; Nakai, H. UV - Visible and ^1H or ^{13}C NMR Spectroscopic Studies on the Specific Interaction between Lithium Ions and the Anion from Tropolone or 4-Isopropyltropolone (Hinokitiol) and on the

https://doi.org/10.1021/jacs.4c14825
J. Am. Chem. Soc. XXXX, XXX, XXX−XXX

Formation of Protonated Tropolones in Acetonitrile or Other Solvents. *J. Phys. Chem. B* **2007**, *111* (7), 1759−1768.
(37) Zhu, F.; Zhang, W.; Liu, H.; Wang, X.; Zhou, Y.; Fang, C.; Zhang, Y. Micro-Raman and Density Functional Theory Analyses of Ion Pairs in Concentrated Sodium Tetrahydroxyborate Droplets. *Spectrochim. Acta, Part A* **2020**, *224* (3), No. 117308.
(38) At concentrations lower than 0.4 mM the experimental values of ion volumes deviate considerably from the theoretical curve. This shows that the equilibrium between free ions and sandwich ion cannot be described by a simple model. However, the concentration limits of DOSY prevent further refinements.
(39) A Database of Published Reactivity Parameters *E*, *N*, and s_N, 2024. https://www.cup.lmu.de/oc/mayr/reaktionsdatenbank2/.
(40) For **4a**, where the anionic sandwich **4a4** dominates, the DOSY measurements show that addition of additive **6** (**a**-BF_4) eventually leads to an inversion of the sandwich ion populations towards the cationic **a4a** (see SI, Chapter 4).

https://doi.org/10.1021/jacs.4c14825
J. Am. Chem. Soc. XXXX, XXX, XXX−XXX